Distribution Agreement

In presenting this thesis as a partial fulfillment of the requirements for a degree from Emory University, I hereby grant to Emory University and its agents the non-exclusive license to archive, make accessible, and display my thesis in whole or in part in all forms of media, now or hereafter now, including display on the World Wide Web. I understand that I may select some access restrictions as part of the online submission of this thesis. I retain all ownership rights to the copyright of the thesis. I also retain the right to use in future works (such as articles or books) all or part of this thesis.

Weigen Yuan April 10, 2015

Giant Magnetoresistance-Like Effect
Observed in a Ferromagnet / Antiferromagnet Bilayer

by

Weigen Yuan

Sergei Urazhdin
Adviser

Department of Physics

Sergei Urazhdin
Adviser

Jasminka Ninkovic
Committee Member

Jed Brody
Committee Member

2015

Giant Magnetoresistance-Like Effect
Observed in a Ferromagnet / Antiferromagnet Bilayer

By

Weigen Yuan

Sergei Urazhdin
Adviser

An abstract of
a thesis submitted to the Faculty of Emory College of Arts and Sciences
of Emory University in partial fulfillment
of the requirements of the degree of
Bachelor of Sciences with Honors

Department of Physics

2015

Abstract
Giant Magnetoresistance-Like Effect
Observed in a Ferromagnet / Antiferromagnet Bilayer
By Weigen Yuan

In our research, we mainly studied the electrical resistance (R) of the ferromagnet / antiferromagnet bilayer film under a changing magnetic field (H), and its dependence on bilayer structures and temperature. By fitting our obtained R v.s. H data with two different functions, we found consistently an asymmetry of the asymptotes at the two extreme positive and negative values of H, when temperature is below 250 K. Although anisotropic magnetoresistance (AMR) was the predominant effect captured by our data, it could not be used to explain this observed asymptotical difference. Instead, an entirely new GMR-like model was proposed to accommodate our experimental data. In addition, we also calculated the effective exchange bias field, H_b, of the F/AF bilayer using two different methods: one is through the fitting function parameter, and the other through original data. When we compared the two calculation results of H_b, we found that they were not in perfect agreement. However, our argument for the GMR-like model should not be compromised by this disagreement of calculated H_b.

Giant Magnetoresistance-Like Effect Observed in a Ferromagnet / Antiferromagnet Bilayer

By

Weigen Yuan

Sergei Urazhdin
Adviser

A thesis submitted to the Faculty of Emory College of Arts and Sciences
of Emory University in partial fulfillment
of the requirements of the degree of
Bachelor of Sciences withHonors

Physics Department

2015

Table of Contents

1 Introduction
1.1General Concepts in Electromagnetism
1.2 Two Types of Magnetism
1.3Hysteresis Loop and Exchange Bias
1.4 Giant Magnetoresistance
1.5Anisotropic Magnetoresistance
2 Equipment and Procedures
3 Analysis Methods
4 Results
5 Discussion
6 Conclusion

1 Introduction

The goal of our research project is to study a giant magnetoresistance(GMR)-like effect on different ferromagnetic (F) / antiferromagnetic (AF) bilayer structures at different temperatures, and thus provide a proof for the existence of this entirely new magnetoresistive effect. More specifically, our focus is to analyze the difference of asymptotic values obtained from function fits on the obtained data. If GMR-like effect indeed exists, such an asymptotical difference is expected to be observed at low temperatures. Also, we could calculate the effective exchange bias field (H_b) with two methods: one by using our data, the other by using the fitting function parameters. If we compare the H_b obtained from these two different methods, we are then able to see if the fitting function itself is well-chosen or not. But before jumping directly into our discussion, we need to clarify some basic terms and concepts which will be often referred to in the following paragraphs.

1.1 General Concepts in Electromagnetism

The very basic concept in electromagnetism is *magnetic dipole moment* (, also called magnetic moment, unit: J/T), defined by how much torque the carrier of the magnetic dipole moment will experience under an applied magnetic field. Magnetic dipole moment in matter mainly arises from either movement or spin of electrons in atoms. Since magnetic dipole moments are usually formed in a huge number in a magnetic material, a vector field called *magnetization* (unit: J/(T*m^3)), M, is devised to describe the density of magnetic dipole moments. (Note: J denotes Joule; T denotes Tesla; N denotes Newton; m denotes meter.)

1.2 Two Types of Magnetism

There are two types of magnetism related to our research: ferromagnetism and antiferromagnetism. These two are different from one another because of their different magnetization configurations. The magnetic moments of a ferromagnetic material (F) tend to align in direction of an applied magnetic field. In additional, the intrinsic magnetic moments tend to align parallel to one other in a neighborhood region, as shown in FIG. 1(a). For a ferromagnet, its magnetic moments will spontaneously orient parallel to one another even without an applied magnetic field. Antiferromagnetism closely resembles ferromagnetism, but the intrinsic magnetic moments, instead of aligning parallel to each other, align anti-parallel to its neighbors, as shown in FIG. 1(b). For an antiferromagnet, there is no net magnetic moment (and thus magnetization), since all of them cancel out.

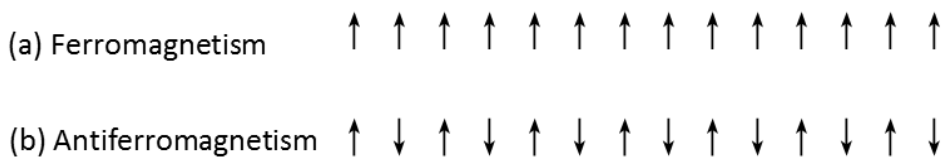

FIG. 1: Two types of magnetic material under non-zero applied magnetic field. (a) Orientation of magnetic moments in a ferromagnetic material. (b) Orientation of magnetic moments in an antiferromagnetic material.

1.3 Hysteresis Loop and Exchange Bias

When a magnetic field is applied to a ferromagnet (F), the magnetization (M) is retained indefinitely around a saturation value, M_S. One may demagnetize the material by reversing the external magnetic field (H), giving rise to a history-dependent relationship between H and M. The magnetic hysteresis loop, shown

in the FIG. 2, captures such a memoristic behavior using an H v.s. M plot.

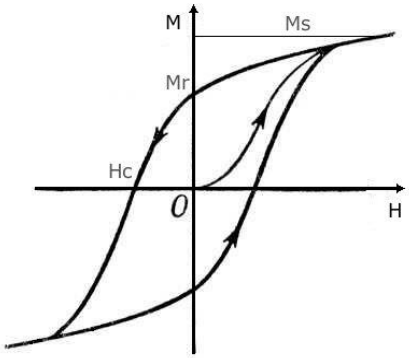

FIG. 2: The H v.s. M plot that shows a hysteresis loop of a typical ferromagnet, with the saturation magnetization, Ms, remnant magnetization, Mr, and coercive field Hc, labeled on the graph. (From Wikipedia, drawn by Ndthe)

The coercivity, also called the coercive field, is the intensity of the applied magnetic field required to reduce the magnetization of the material to zero from its saturation value.

Unlike ferromagnetic material that has a symmetric hysteresis loop, an F/AF bilayer typically exhibit an asymmetric hysteresis loop under an applied magnetic field. Such an asymmetry is usually characterized by the effective exchange bias field, H_b.

In a microscopic view, the origin of exchange bias is the exchange-coupling of magnetization at F and AF interface. When one cools the F/AF system under a magnetic field, the M of F is exchange-coupled to the frozen M of AF. Since this exchange-coupling has the interfacial spins of F pinned to AF, an additional energy must be added to break the strong coupling between the two magnets, in order to reverse the magnetic moments in F under a non-zero magnetic field. The shift of hysteresis loop from H=0 axis to H_b is solely a manifestation of such an energy compensation, shown in FIG. 3 c) below

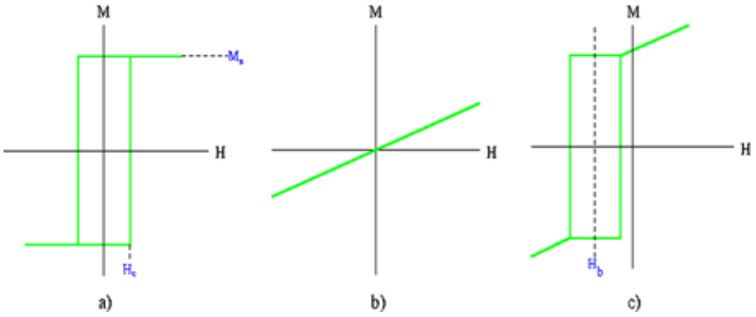

FIG.3: Hysteresis loops for three different magnetic materials. a) Hysteresis loop of a ferromagnet; Saturation magnetization, Ms, and coactivity, H_c, are labeled on the plot. b) Linear relationship between M and H for an antiferromagnet. c) Shifted hysteresis loop of an F/AF bilayer; H_b is labeled on the plot. (Note: The slope of magnetization curve of AF is exaggerated for clarity.) (From Wikipedia, drawn by Alison Chaiken using Xfig)

1.4 Giant Magnetoresistance

Giant magnetoresistance (GMR) is a magnetoresistive effect in film structures of alternating non-magnetic conductive layers (NM) and ferromagnetic layers (FM), as shown in FIG. 4 on right. According to GMR theory, if the magnetizations of neighboring ferromagnetic layers are parallel, the electrical resistance (R) will be relatively low; if the magnetizations are anti-parallel, R will be relatively high, shown in FIG. 4 on right. In other words, GMR characterizes the dependence of R on adjacent FM layers' magnetizations.

Generally, magnetoresistance describes the electrical resistance change of a material due to a change of

the strength of external magnetic field. Magnetoresistance is expressed mathematically as

$$\delta_H = [R(0) - R(H)] / R(H) \quad (1)$$

where R(H) is the resistance of the material under an external magnetic field H, and R(0) is the resistance of the material under zero external magnetic field. Some examples of GMR plots are shown in FIG. 4 on left. The reason why "giant magnetoresistance" is chosen to name this effect is that the value δ_H for GMR-structured films is considerably larger (nearly 80% difference between the maximum and minimum resistance) than most of the magnetoresistive effects, such as anisotropic magnetoresistance, which is the subject of the next section.

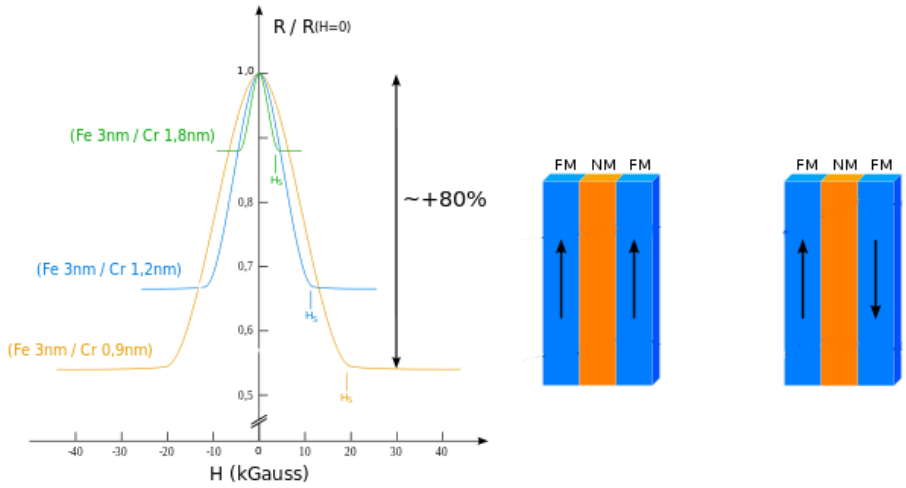

FIG. 4: Left: GMR of some typical multilayer structures; the maximum GMR and minimum GMR can differ up to nearly 80%. Right: General structure of alternating non-magnetic conductive layers (NM) and ferromagnetic layers (FM) film, with two magnetization configuration, labeled. (From Wikipedia, uploaded by Igge)

1.5 Anisotropic Magnetoresistance

Anisotropic magnetoresistance (AMR) characterizes the change of electrical resistance of a material due to an angle difference between the direction of electric current (I) and the direction of the magnetization (M) of the material. For most magnetic materials, electrical resistance (R) reaches its maximum when M orients parallel to I, and its minimum when the two have directions perpendicular to one another. FIG. 5 below shows the resistance of a CoO(8)Py(10)SiO_2(10) thin film varies as a function of the angle under an applied magnetic field at room temperature.

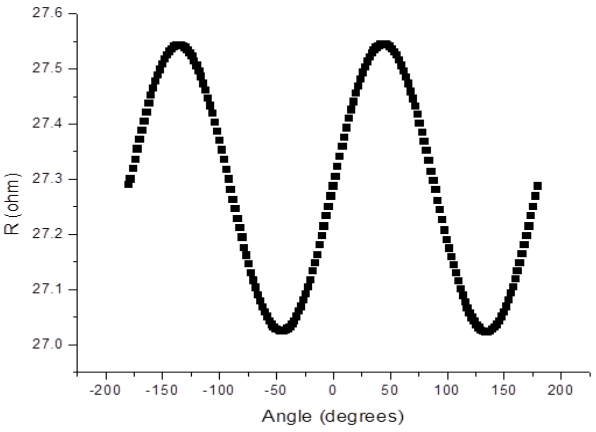

FIG. 5: AMR plot for a CoO(8)Py(10)SiO_2(10) thin film at temperature of 300K under an applied magnetic field of 2500 Oe. The R varies sinusoidally with a 180-degree period.

2 Equipment and Procedures

By using a high-vacuum sputtering machine, our samples can be deposited with different thicknesses of Py (ferromagnetic) and CoO (antiferromagnetic) on a SiO_2 thin film at room temperature, to build a desired F/AF bilayer. The samples that we are going to study have only the thickness of Py varied, at 5, 10, and 20 nm respectively, while keeping the same thickness of CoO at 8nm. The thickness of SiO_2 thin film is 10nm.

To perform a magnetoelectronic characterization on the sample films, we used the four-probe van der Pauw geometry, with an alternating current (AC) source I = 0.3 mA at frequency f = 1.3 kHz. A lockin is used to detect the AC voltage on the film, and thus give the resistance across the F/AF bilayer film. The film sits fixed in a chamber, and the direction current is fixed relative to the film. Only the magnet can be rotated and thus change the direction in which the magnetic field is applied onto the film.

The first step was to rotate the magnet so that R was minimized under the H (in our case, 100 Oe) at room temperature. We performed this procedure because R is lowest when the directions of I and M are perpendicular to each other, according to AMR theory. This configuration of M and I will make our analysis easier later on, because any fluctuation of M will cause an increase in R. It is worth noticing that the direction of current I is fixed, while the direction of M is the same as the direction of H.

Next, we cooled the system from 300 K to 5.5 K under a constant magnetic field of 500 Oe without changing the direction of the magnet. This second step enabled us to set up an exchange bias at the F/AF interface, when it is cooled through a blocking temperature, Tb, in the presence of an applied magnetic field. Tb typically has a value that is close to or lower than the Néel temperature, Tn of the AF. The Tn of CoO, used in our bilayer structure, is 291 K.

After the temperature was stabilized, by changing the strength and switching the direction of the magnetic field from -9000 Oe to 9000 Oe, we collected the AMR data, which yielded a relationship between H and R. We performed this same measurement at each stabilized temperature point from T = 5.5 K to T = 300 K at a 20-K interval, for each of the three structures of F/AF bilayers: CoO(8)Py(5)SiO_2(10), CoO(8)Py(10)SiO_2(10), and CoO(8)Py(20)SiO_2(10) (unit is nanometer).

3 Analysis Methods

Our analysis of the obtained AMR data is mainly on 1) collecting the asymptotic difference and 2) calculating the effective exchange bias field, H_b, from obtained data plot. To achieve these two goals, we first need to find a fitting function. Specifically, we need a function that does not only fit our experimental data, but also has a well-defined physical interpretation for each of its parameter. To avoid confusion, let's denote the applied magnetic field to be H, and the angle formed by the magnetization (M) of permalloy relative to this applied magnetic field to be Φ. We define H_{tot} to be the net effective magnetic field, including both the applied field and the effects of the exchange interaction with AF. The direction of H_{eff} determines the direction of M. $H'_{\parallel}$ and $H'_{\perp}$ are average components of the effective exchange field H′, with $H'_{\parallel}$ in the direction of H and $H'_{\perp}$ perpendicular to the direction of H. It is usually easy to be confused by the terminology in many literatures, so let's make it clear that H′ stands for *effective exchange field*, while $H'_{\parallel}$ (also written as H_b) stands for *effective exchange bias field*. FIG. 6 is a clear presentation of all parameters mentioned above.

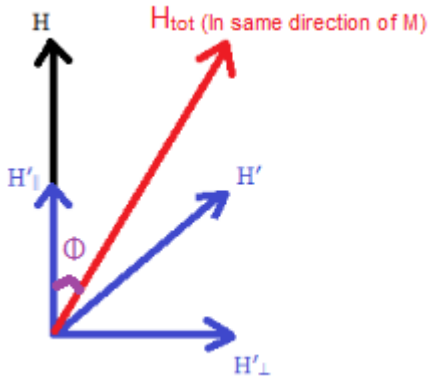

FIG. 6: Fields and magnetizations of F/AF bilayer under an applied magnetic field. H is the external magnetic field; H′ is the effective exchange field; $H'_{\parallel}$ and $H'_{\perp}$ are components of H′ in direction of H and perpendicular to it; H_{tot} is the net magnetic field of the system, which is in the same direction of the magnetization of Py. (Note: $H_b = H'_{\parallel}$)

Because of trigonometry, sin(Φ) can be expressed as

$$\sin(\Phi) = H'_{\perp} / (H + H'_{\parallel}) \quad (2).$$

By small angle approximation, we know that

$$\sin(\Phi) \approx \Phi \quad (3).$$

We also define ΔR as

$$\Delta R = R(90^{o}) - R(0^{o}) \quad (4)$$

, where $R(90^{o})$ is the maximum resistance when the current is applied parallel to M, and $R(0^{o})$ the minimum resistance when current is applied perpendicular to M, according to the AMR theory. It is indicated by Professor S. Urazhdin's most recent paper that the resistance of an F/AF bilayer should be

$$R = R_{min} + (\Delta R / 2) * \Phi\text{^}2 \quad (5)$$

, where R_{min} is resistance minimum at Φ = 0. Equation (5) can also be rewritten as

$$R = R_{min} + (\Delta R / 2) * [H'_{\perp} / (H + H'_{\parallel})]\text{^}2 \quad (6),$$

which is one of the equations that we used to fit our measured data plot.

4 Results

Following the experiment procedures described earlier, we obtained the R v.s. H data plot at each temperatures for each bilayer structure. Let's focus on the data for the bilayer film CoO(8)Py(5)SiO_2(10). At base temperature T = 5.5K (shown in FIG. 7, upper left), as the applied magnetic field (H) changes from -9000 Oe to 1000 Oe, there is a non-linear increase of resistance (R). After a sudden decrease of R around H = 1000 Oe, R keeps decreasing non-linearly and finally approaches its asymptotical value under a large positive magnetic field, H = 9000 Oe in our case. (Note: negative sign of H indicates that the magnetic field is applied in the opposite direction of +H.) As the magnetic field decreases from 9000 Oe to -9000 Oe, the trending curve of R mirrors the previous one except that the asymptotical values are fixed at the two extreme positive and negative H values.

Now compare the data plots for CoO(8)Py(5)SiO_2(10) bilayer film at different temperatures. As the temperature increases from 5.5 K to 300 K, the H at which R drops shrinks towards zero, shown in FIG. 7. At T = 5.5 K, a difference of asymptotical values on the right side and the left side seems to exist under bare-eye observation. If one observes FIG.7 more carefully, one can roughly estimate that the asymptotical difference at two tails of a data plot decreases as the temperature rises, since the scales of the plots in FIG. 7 are more or less the same.

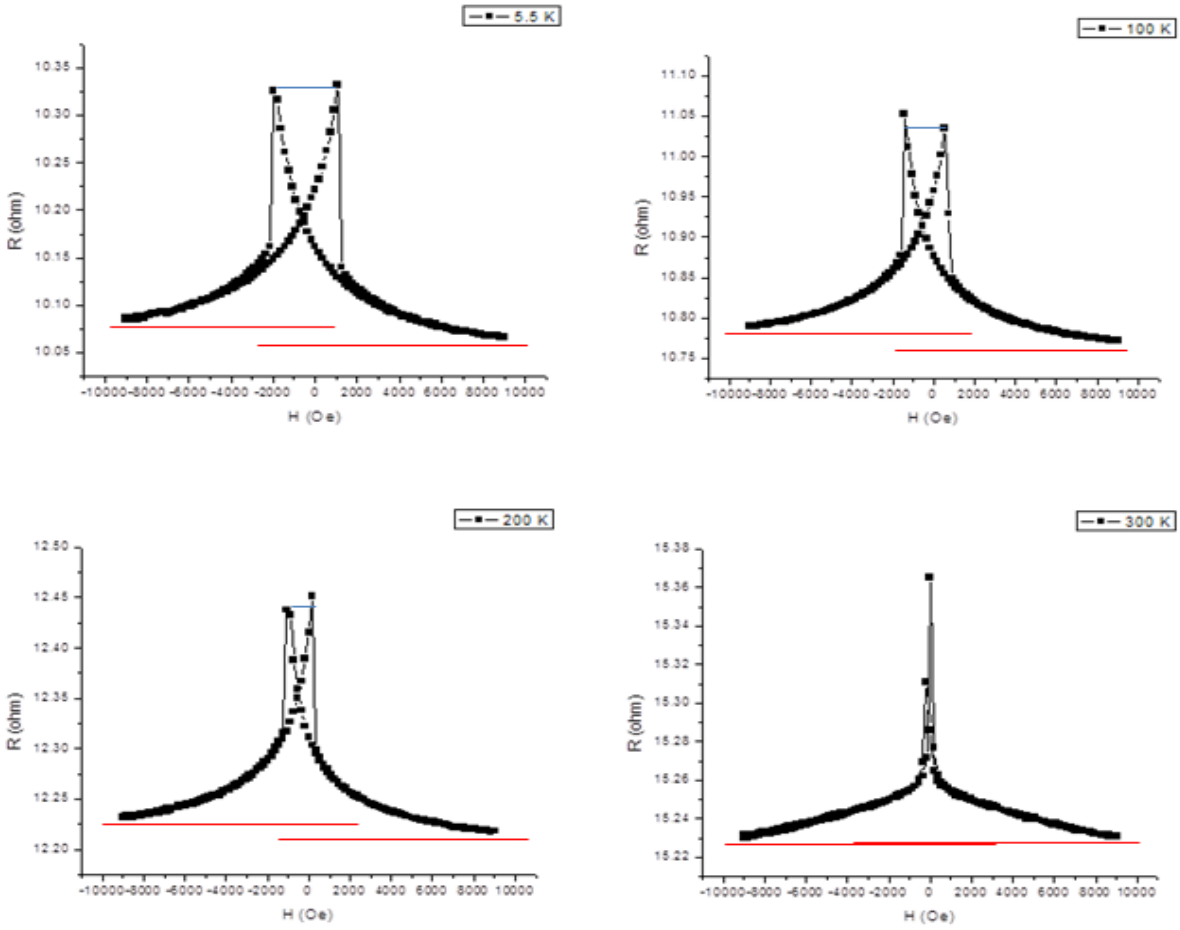

FIG. 7: R v.s. H data plots for bilayer film CoO(8)Py(5)SiO_2(10) at different temperatures. Upper left: the data plot at T = 5.5 K. Upper right: the data plot at T = 100 K. Lower left: the data plot at T = 200 K. Lower right: the data plot at T = 300 K. The horiztonal blue lines that connect the peaks are used to visually compare the H, where R has a sudden drop, at different temperatures. At T = 5.5 K, the length of the blue line is abot 2000 (Oe); at T = 100 K, the length of the blue line is abot 1000 (Oe); at T = 200 K, the length of the blue line is abot 400 (Oe); at T = 300 K, the length of the blue line is abot 30 (Oe). The horizontal red lines are roughly estimated asymptotes of the curves in the plots.

A direct visual presentation of the scales of resistance at different temperatures is shown in FIG. 8. One can also clearly see the decrease of H, at which R has a sudden drop around H = 0 in FIG. 8. The data plots for CoO(8)Py(10)SiO_2(10) and CoO(8)Py(20)SiO_2(10) bilayer films are similar to the ones displayed, only with different scales.

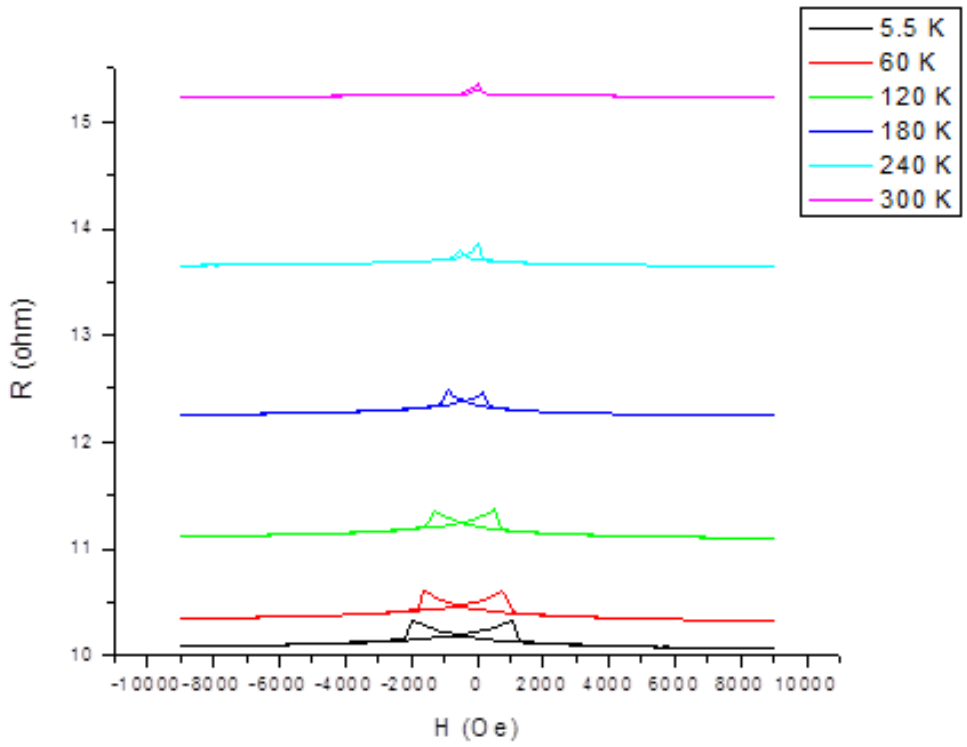

FIG. 8: R v.s. H data plots for bilayer film CoO(8)Py(5)SiO_2(10) at different temperatures. From lowest to the highest, the data plot curves are obtained at T = 5.5K in black, T = 60 K in red, T = 120 K in green, T = 180 K in blue, T = 240 K in light blue, T = 300 K in pink.

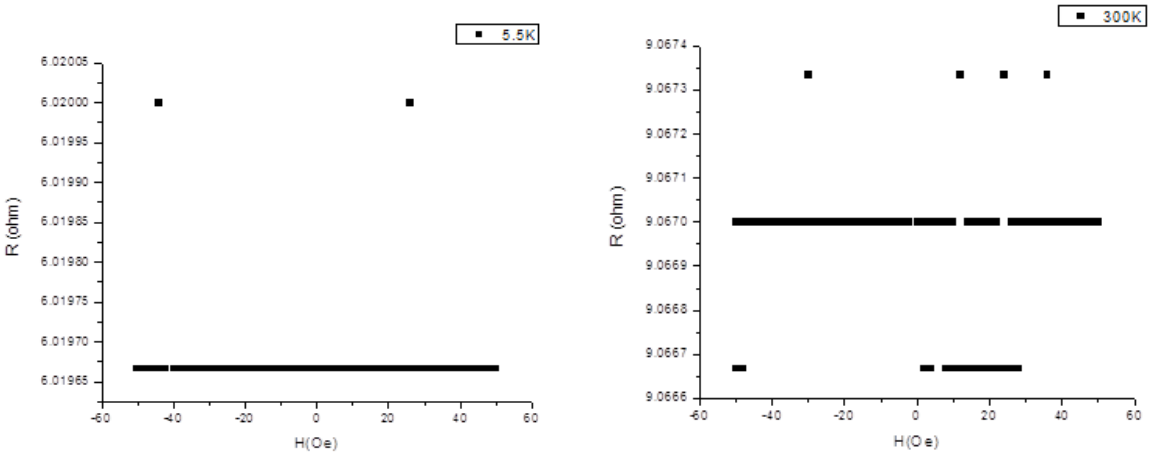

FIG 9: R v.s. H plot for Py(10)SiO_2(10) thin film. Rght: data plot of the film at T = 5.5 K. Left: data plot of the film at T = 300 K.

In order to make sure our measurement of R v.s H is not flawed, we made a Py(10)SiO_2(10) thin film and carried out the same procedure we used in the earlier measurements. As expected, the R remains constant as the magnetic field changes, shown in FIG. 9. This shows that a standalone F single layer film cannot cause the GMR-like effect observed in an F/AF bilayer film. The outliers might result from noise when measurements were taken.

5 Discussion

In order to study the asymptotical difference of the data at large H, we need to find a function that can best fit our obtained data. We tried two functions in our analysis.

The first one is in form: $y = a + b / (x + c)$. This is an emprical fitting function because no good interpretation of the parameters could be given. In our analysis, we always fitted twice for each data plot, because the H changes from -9000 Oe to 9000 Oe and back again to -9000 Oe. In particualr, for each "H scan" (H from nagtive to positive value, or the other way around), we were only interested in fitting the part of curve that has a smooth nonlinear increase or decrease. And since we "scanned" twice for each plot, there will be two smooth nonlinear curves to be fitted. For the emprical fitting function, parameter *a* tells us the asymptotical values; parameter *b* and *c* are not fixed when we did fitting iterations. For CoO(8)Py(5)SiO_2(10) bilayer film, as shown in FIG. 10 upper left, this emprical function fits our data nicely at low temperature, with R^2 = 0.99992. however it falls off from our data as the temperature rises above 240 K, shown in FIG. 11 upper right, with R^2 = 0.99081. The other two structures have similar fitting results.

The second function that we used is in form: $y = a - b / [(1 + c * x) \wedge (1 / d)]$, and let's call it an *analytic function*. By matching up this analytic function with equation (6), one can easily derive that $a = R_{min}$, $b = -(\Delta R / 2) * (H'_{\perp} / H'_{\parallel})^2$, $c = 1 / H'_{\parallel}$, $d = 0.5$, x = H. Since H′ cannot be dermined directly from our data, parameter *b* and *c* are not fixed when we did fitting iterations; parameter *a* tells us the asymptotical values. As shown in FIG. 10 lower left, this analytic function also fits our data nicely at low temperature, with R^2 = 0.99884. However, just like the emprical one, the analytic fitting fail as the temperature rises above 220 K, with R^2 = 0.97947, shown in FIG. 11 upper right. The other two structures have similar fitting results as well.

Now we are ready to verify the bare-eye observed dependence of the asymptotical difference (dR) on temperature (T). By using both empirical and analytic function, we fitted all data plots at different temperatures for different bilayer structures, and sorted out the asymptotical values, making them into dR v.s. T plots. For CoO(8)Py(5)SiO_2(10) bilayer structure, both fitting functions yield the same result that dR tends

to decrease as T rises, shown in FIG. 11 upper left (empirical) and right (analytic). To make a better comparison, dR / R is used to cancel out the scaling factor, as shown in FIG. 11 lower left (empirical) and right (analytic). In a similar fashion, for CoO(8)Py(10)SiO_2(10) bilayer structure, the two fitting functions still yield the same general decreasing trend of dR as T rises, shown in FIG. 12. For CoO(8)Py(20)SiO_2(10) bilayer structure, however, a general increasing trend of dR is found using both fitting functions, shown in FIG 13. The nonmonotonic decrease/increase might result from the limit of fitting precision, or the unstableness of the temperature while measurements were taken. Despite these bizarre bumps in these dR v.s. T plots, we still can conclude the evidence of dR with confidence.

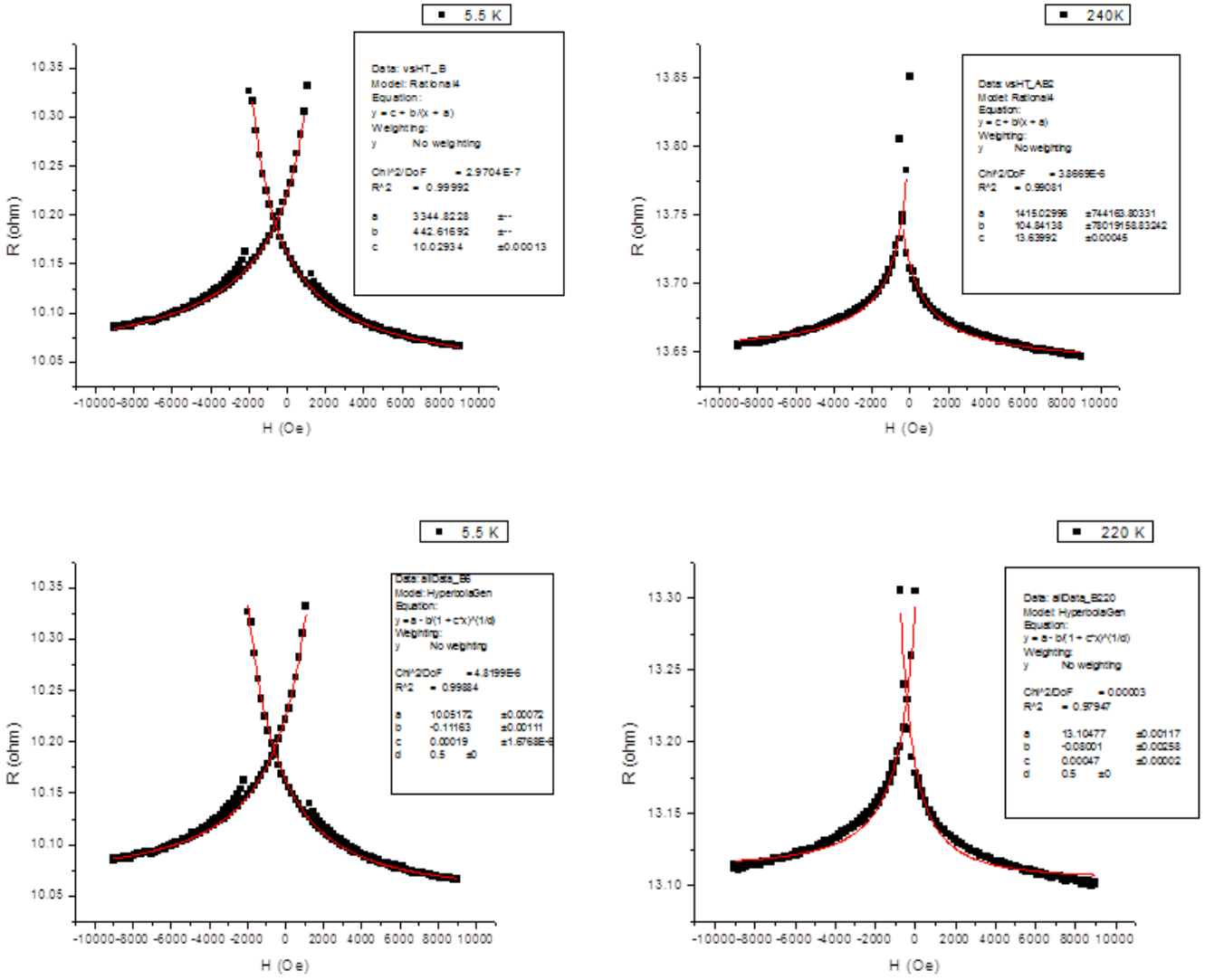

FIG. 10: Fitting of data plots for bilayer film CoO(8)Py(5)SiO_2(10) by empirical and analytic functions. Upper left: the data plot fitted by empirical function at T = 5.5 K, R^2 = 0.99992. Upper right: the data plot fitted by empirical function at T = 240 K, R^2 = 0.99081. Lower left: the data plot fitted by empirical function at T = 5.5 K, R^2 = 0.99884. Lower right: the data plot fitted by empirical function at T = 220 K, R^2 = 0.97947. The empirical function has form: $y = c + b / (x + a)$; the analytic function has form: $y = a - b / [(1 + c * x) \wedge (1 / d)]$.

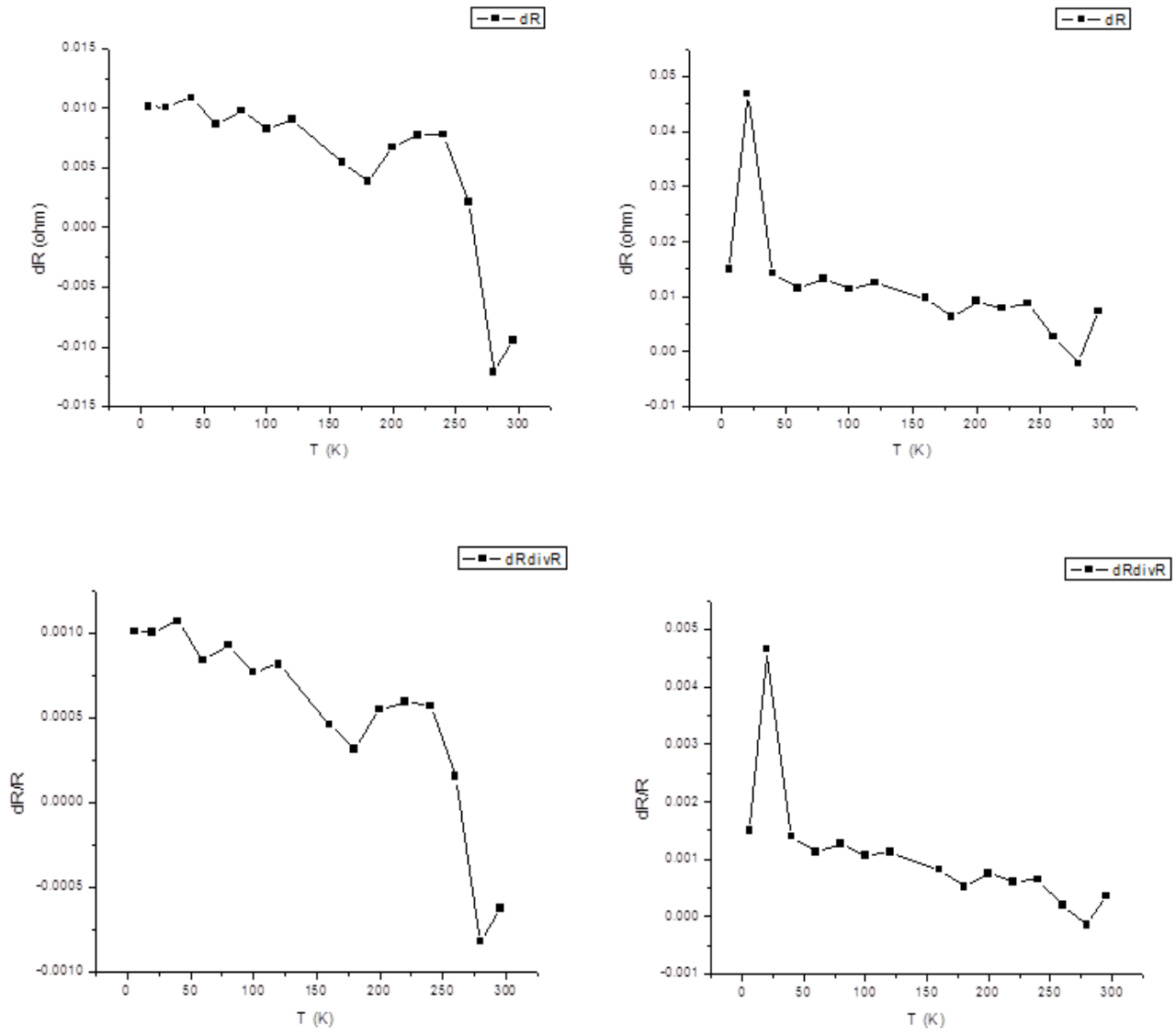

FIG. 11: The dependence of asymptotical difference on temperature for bilayer film CoO(8)Py(5)SiO_2(10). Upper left: dR v.s. T, obtained from empirical fitting function. Upper right: dR v.s. T, obtained from analytic fitting function. Lower right: dR/R v.s. T, obtained from empirical fitting function. Lower left: dR/R v.s. T, obtained from analytic fitting function.

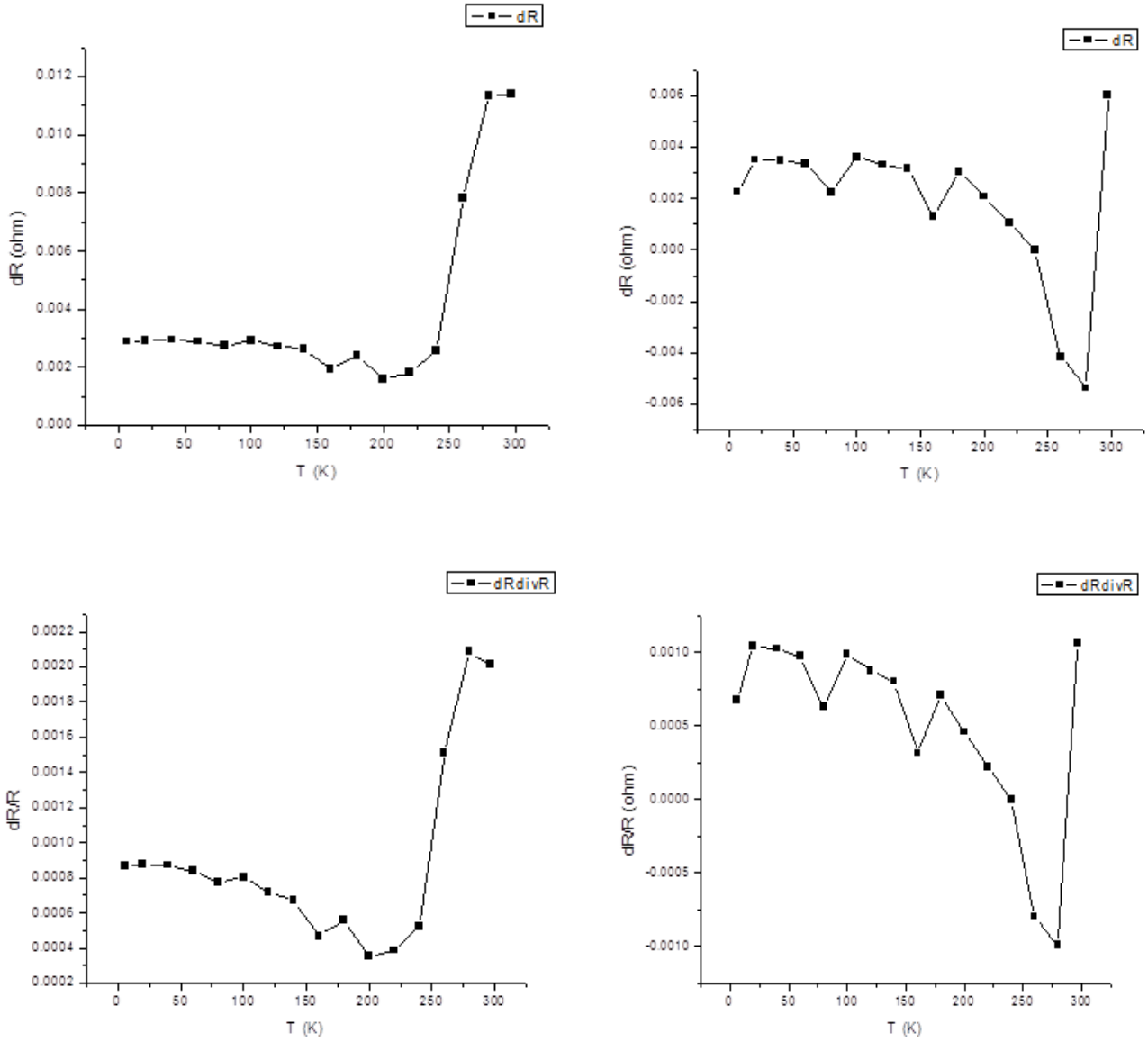

FIG. 12: The dependence of asymptotical difference on temperature for bilayer film CoO(8)Py(10)SiO_2(10). Upper left: dR v.s. T, obtained from empirical fitting function. Upper right: dR v.s. T, obtained from analytic fitting function. Lower right: dR/R v.s. T, obtained from empirical fitting function. Lower left: dR/R v.s. T, obtained from analytic fitting function.

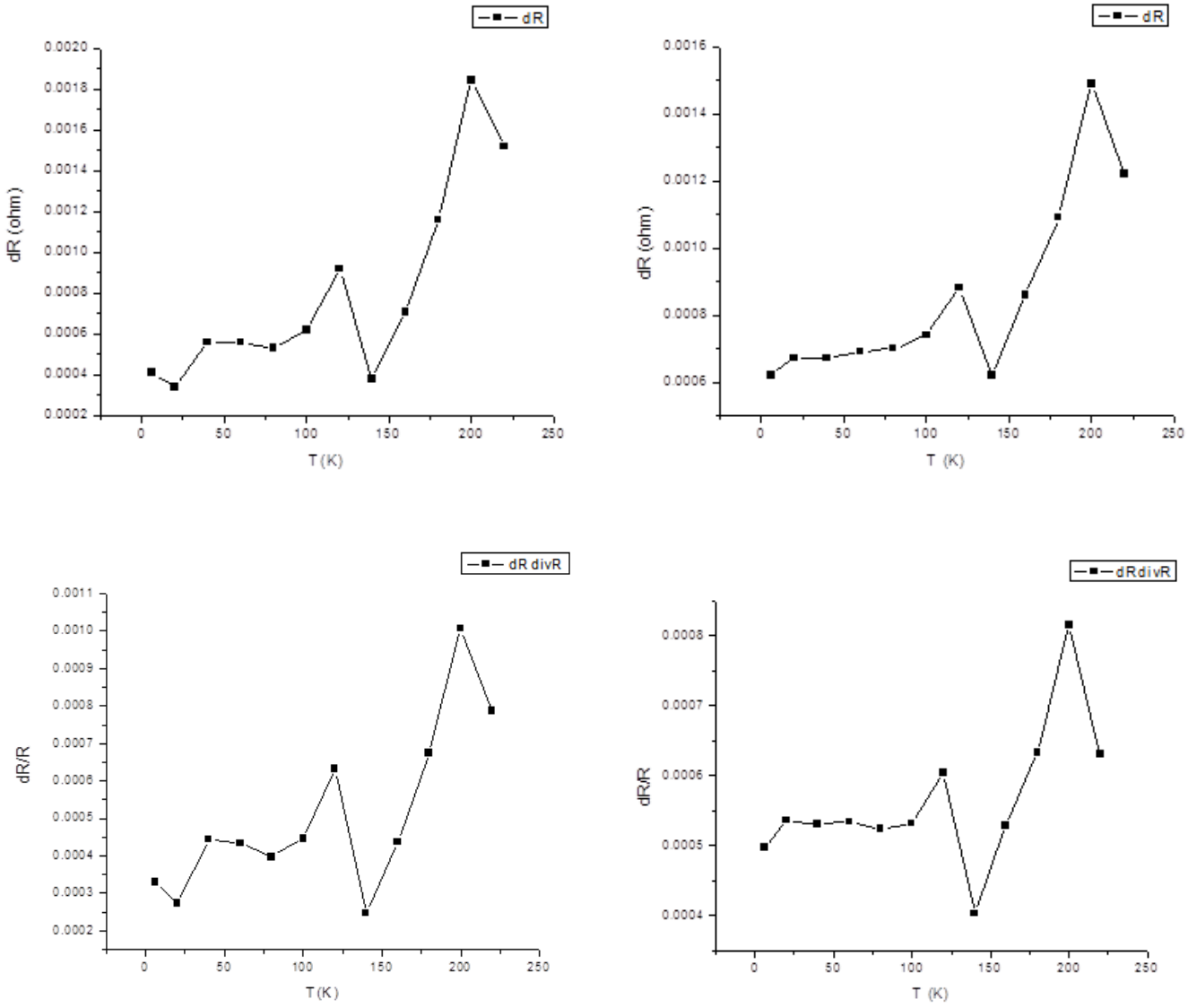

FIG. 13: The dependence of asymptotical difference on temperature for bilayer film $CoO(8)Py(20)SiO_2(10)$. Upper left: dR v.s. T, obtained from empirical fitting function. Upper right: dR v.s. T, obtained from analytic fitting function. Lower right: dR/R v.s. T, obtained from empirical fitting function. Lower left: dR/R v.s. T, obtained from analytic fitting function.

The reason why we want to see this solid evidence of dR is that it cannot be explained by AMR, even though our obtained data are predominantly due to AMR effect. It is true that if the applied magnetic field (H) were not large enough, the magnetization (M) of F layer would not be saturated, giving rise to a M component that is perpendicular to H and thus parallel to current (I) in our case. According to AMR theory, this M component will cause a larger R rather than its minimum, which might be an explanation for the observed dR. However, we have two reasons to dispel this AMR model. First, in our experiment, we made H as large as 9000 Oe, which is almost 1 tesla, bringing the angle Φ of the magnetization very close to zero. Second, since we used asymptotes to yield this dR, and by definition asymptotical values of R is at H = ∞ instead of some finite H, AMR should not be the reason why dR is observed.

Here, we propose a GMR-Like model as the explanation of the observed asymptotical difference, dR. We know that at the interface of F/AF bilayer, there are two possible exchange-coupling configurations, shown in FIG. 14 on bottom left and bottom right. It is well-known that exchange bias is associated with uncompensated AF magnetic moments at the interface with F. Comparing the top schematics in Fig.14 for the well-established GMR effect involving two magnetic layers, with the bottom schematic for a single F/AF bilayer, we can see that these uncompensated spins can play the role of the second F, resulting in a GMR-like effect.

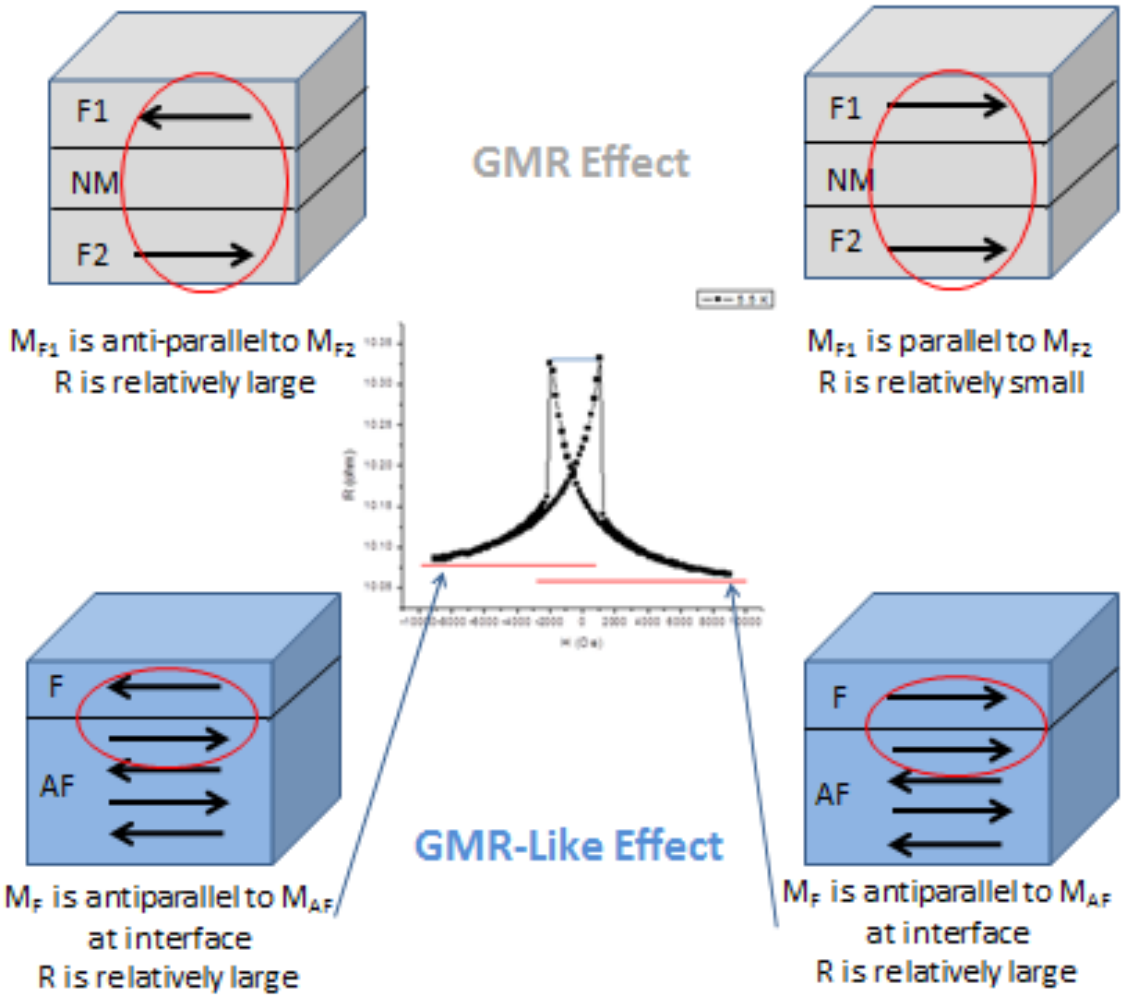

FIG. 14: Comparison between GMR effect and GMR-like effect. Upper part: GMR structured films with alternating ferromagnetic layers (F1, F2) and conductive non-magnetic layer (NM). Two possible magnetization (M) configurations of F1 and F2 are labeled. Lower part: F/AF bilayer film with an F layer and an AF layer. Two possible M configurations at F and AF interface are labeled. Middle part: obtained data plots for bilayer film CoO(8)Py(5)SiO_2(10) at T = 5.5 K; approxiamted asysmptotes are labeled. The red circles are drawn to mark out the similarity of M configurations between the two differently structured films vertically.

As our second goal, we also managed to calculate the effective exchange bias field, H_b, with two

different methods, and by comparing the results of these two methods, we can conclude whether our equation (6) is a good or bad fitting function for F/AF system.

The first method that we used to calculate H_{b1} (, the calculated effective exchange bias field using the first method,) is by finding the two coercive fields from the hysteresis loop of F/AF film, and then calculating the numeric mean of these two values. Although we do not have the usual M v.s. H hysteresis loop plot to locate the coercive fields, we can still know their values from our R v.s. data. This is because the value of H corresponding to the resistance peak is actually the coercive field in an M v.s. H data. With little difficulty, we calculated H_{b1} at different temperatures for different bilayer structures, and presented it in FIG. 15. For all plots in FIG. 15, H_{b1} always go to zero as temperature rises to room temperature, since the exchange bias disappears above the blocking temperature, Tb. The scales of the plots are also decreasing, from 1600 Oe to 200 Oe as the thicknesses of Py increase in the bilayer structure. This is also expected, because the thicker the F layer relative the AF layer is, the weaker is the effective exchange field produced by the exchange coupling at the F/AF interface

The second method used to calculate H_{b2} (, the calculated effective exchange bias field using the second method,) is to use the fitting parameter c of the analytic function, with equation $c = 1 / H'_{\|}$. Because we ftted twice for each data plot, there should be two values of c as well, for example $c1$ and $c2$ (, of which one should be positive and one shuold be negative). Then we can obtain the effective exchange bias field, which is simply $H_{b2} = (1 / c1) + (1 / c2)$. After sorting out our data, we calculated H_{b2} and plotted it with H_{b1}, as shown in FIG. 16.

After comparing the two calculated results of H_b using two different methods in FIG. 16, one can see that only the plot (b) has a relatively good agreement between H_{b1} and H_{b2} at lower temperature. For plot (a), H_{b1} and H_{b2} are always in trend of one another, but a difference of their quantitative values persists. For plot (c), H_{b1} and H_{b2} are neither in trend with one another, nor is their difference small enough to prove equation (6) is an ideal mathematic model for the F/AF system.

As a whole, even though we cannot conclude the equation (6) is a well-chosen mathematic model for the F/AF bilayer system, we still see some correspondence between the parameters and the real physical quantities. A more in-depth study of the subject should bring some light onto the complication we had here.

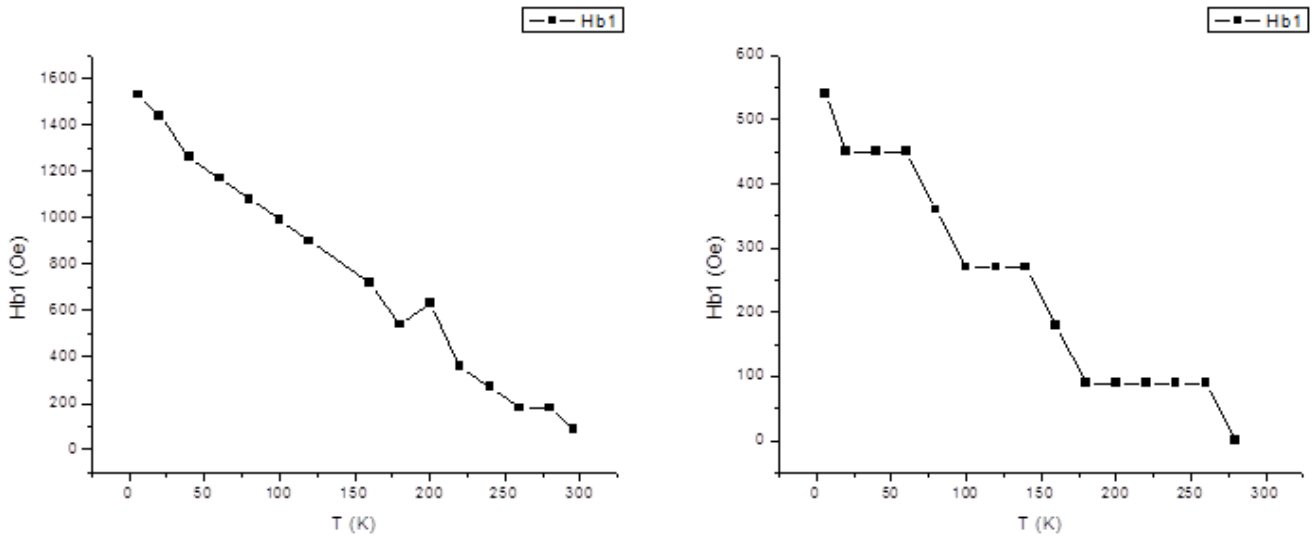

(a) **(b)**

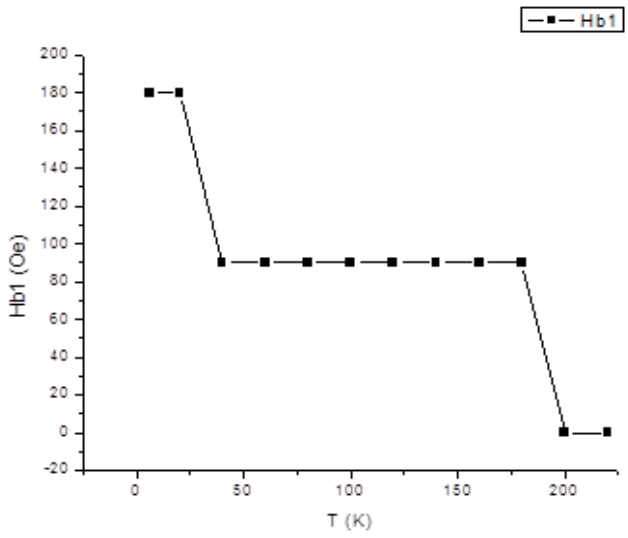

(c)

FIG. 15: Effective exchange bias fields calculated using the first method for different F/AF structures at different temperatures. (a): H_{b1} v.s. T plot for CoO(8)Py(5)SiO_2(10) thin film. (b): H_{b1} v.s. T plot for CoO(8)Py(10)SiO_2(10) thin film. (c): H_{b1} v.s. T plot for CoO(8)Py(20)SiO_2(10) thin film. Note: H_{b1} is the calculated exchange bias field using the first method described in the paragraph.

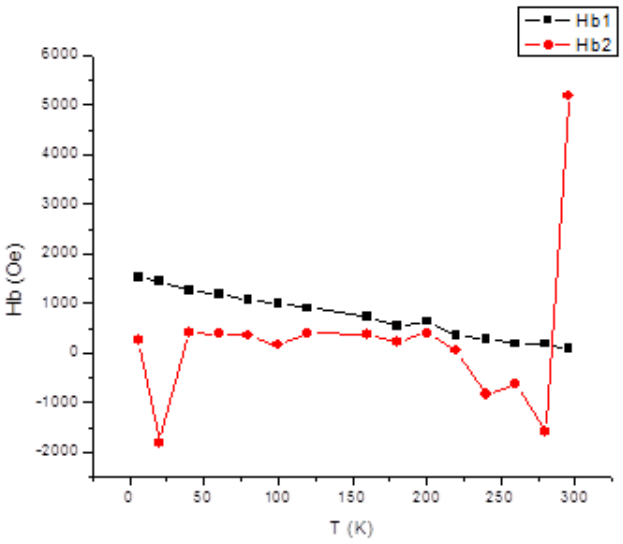

(a)

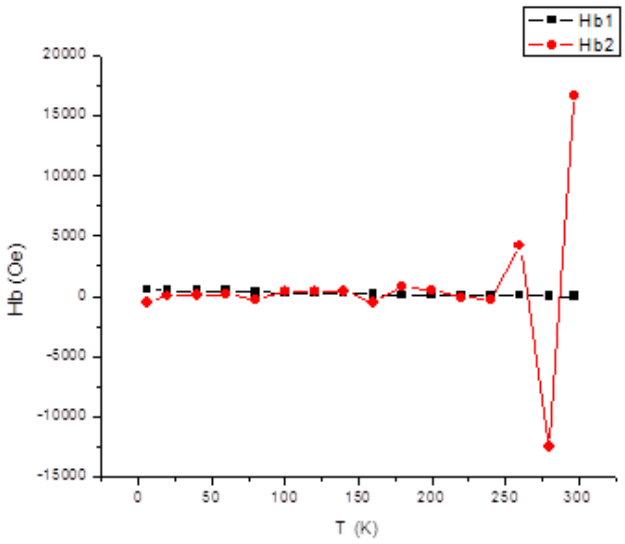

(b)

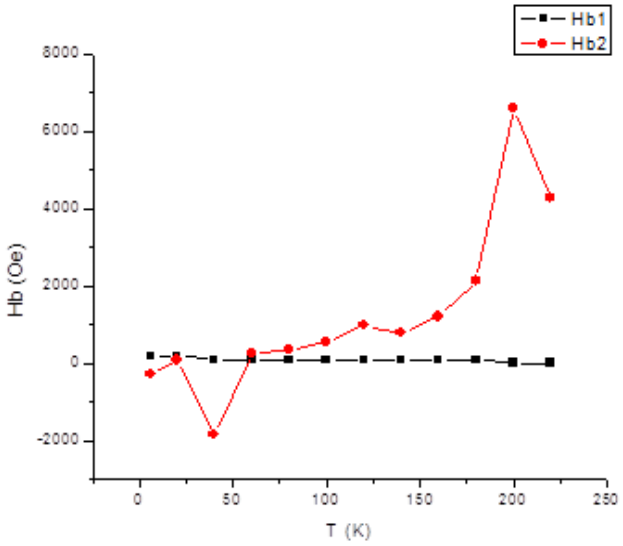

(c)

FIG. 16: Effective exchange bias fields calculated using the first and the second method for different F/AF structures at different temperatures. (a): For $CoO(8)Py(5)SiO_2(10)$ thin film, H_{b1} v.s. T is plotted in black lines, and H_{b2} v.s. T is plotted in red lines. (b): For $CoO(8)Py(10)SiO_2(10)$ thin film, H_{b1} v.s. T is plotted in black lines, and H_{b2} v.s. T is plotted in red lines. (c): For $CoO(8)Py(5)SiO_2(20)$ thin film, H_{b1} v.s. T is plotted in black lines, and H_{b2} v.s. T is plotted in red lines. Note: H_{b2} is the calculated exchange bias field using the second method described in the paragraph.

6 Conclusion

In our research, we mainly studied the electrical resistance (R) of the F/AF bilayer film under a changing magnetic field (H), and its dependence on bilayer structures and temperature (T).

Following the experiment procedures, we obtained the R v.s. H data at different temperatures for different F/AF bilayer structures. By fitting our obtained R v.s. H data with two different functions, we found consistently an asymmetry of the asymptotes at the two extreme positive and negative values of H, when T is below 250 K. Since such an asymptotical difference could not simply result from AMR effect, we proposed an entirely new GMR-like model to accommodate our experimental result. This new model makes good sense, because the uncompensated spins of AF layer can play the role of the second F in GMR, when the bilayer system is under the blocking temperature of AF, which is close to or lower than the Néel temperature of CoO at 291 K.

In addition, we also calculated the effective exchange bias field, Hb, of the F/AF bilaye using two different methods: one is through the fitting function parameter, and the other through original data. When we compared the two calculation results of Hb, we found that they were not in perfect agreement. However, our argument for the GMR-like model should not be compromised by this disagreement of calculated Hb.

Reference

[1] Urazhdin, Sergei. "ArXiv.org Cond-mat ArXiv:1503.08380." [1503.08380] Cooperative Multiscale Aging in a Ferromagnet/Antiferromagnet Bilayer. N.p., 29 Mar. 2015. Web.

[2] Baibich, M. N.; Broto; Fert; Nguyen Van Dau; Petroff; Etienne; Creuzet; Friederich; Chazelas (1988). "Giant Magnetoresistance of (001)Fe/(001)Cr Magnetic Superlattices."Physical Review Letters. N.p., 21 Nov. 1988. Web.

[3] Bertotti, Giorgio. Hysteresis in Magnetism: For Physicists, Materials Scientists, and Engineers. San Diego: Academic, 1998. Print.

[4] Camley, R. E. and Barnaś, J. "Theory of Giant Magnetoresistance Effects in Magnetic Layered Structures with Antiferromagnetic Coupling." Physical Review Letters. N.p., 07 Aug. 1989. Web.

[5] Coey, J. M. D. Magnetism and Magnetic Materials. Cambridge: Cambridge UP, 2009. Print.

[6] Cullity, B. D. Introduction to Magnetic Materials. Reading, MA: Addison-Wesley Pub., 1972. Print.

[7] De Ranieri, E.; Rushforth, A. W.; Výborný, K.; Rana, U.; Ahmed, E.; Campion, R. P.; Foxon, C. T.; Gallagher, B. L.; Irvine, A. C.; Wunderlich, J.; Jungwirth, T. "ArXiv.org Cond-mat ArXiv:0802.3344." [0802.3344] Lithographically and Electrically Controlled Strain Effects on Anisotropic Magnetoresistance in (Ga,Mn)As. N.p., 22 Feb. 2008. Web.

[8] Fert, A. "Nobel Lecture: Origin, Development, and Future of Spintronics." Reviews of Modern Physics. N.p., 17 Dec. 2008. Web.

[9] Kiwi, Miguel (September 2001). Exchange Bias Theory. N.p., Sept. 2001. Web. 02 Apr. 2015.

[10] Mayergoyz, Isaak D. Mathematical Models of Hysteresis and Their Applications. Amsterdam: Elsevier, 2003. Print.

[11] McGuire, T.; Potter, R. "Anisotropic Magnetoresistance in Ferromagnetic 3d Alloys." IEEE Xplore. N.p., June 2003. Web.

[12] Meiklejohn, W. H.; Bean, C. P. "New Magnetic Anisotropy." APS Journals. N.p., 01 Feb. 1957. Web.

[13] Nogués, J.; Ivan K. Schuller. Exchange Bias. N.p., 15 Feb. 1999. Web.

[14] P. Wiśniewski, "Giant Anisotropic Magnetoresistance and Magnetothermopower in Cubic 3:4 Uranium Pnictides." Giant Anisotropic Magnetoresistance and Magnetothermopower in Cubic 3:4 Uranium Pnictides. N.p., 8 May 2007. Web.